JOC Article

Substituent Effects on Tandem Alkenyl Migration/Electrophilic Aromatic Substitution Reactions: A Theoretical Study

Selina C. Wang and Dean J. Tantillo*

Department of Chemistry, University of California, Davis, One Shields Avenue, Davis, California 95616

tantillo@chem.ucdavis.edu

Received July 15, 2007

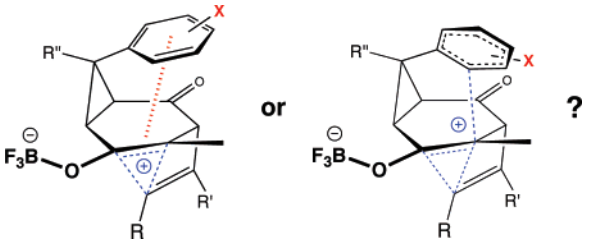

Quantum mechanical calculations (B3LYP/6-31G(d)) were used to study the substituent effects and the concertedness of the alkenyl migration/electrophilic aromatic substitution reactions recently reported by Oshima and co-workers. Our calculations suggest that these systems prefer stepwise mechanisms with their aryl attack steps having the highest energy transition structures, but that in some highly substituted cases, effectively concerted but very asynchronous processes may occur.

Introduction

Recently, Oshima and co-workers described the intriguing rearrangement reaction shown in Scheme 1, which efficiently assembles a complicated polycyclic architecture via an alkenyl migration/electrophilic aromatic substitution process.[1,2] It was suggested by these authors that the [1,2] alkenyl migration and aryl attack steps in this process may be concerted (Scheme 2, mechanism A).[1] This conclusion was largely based on the comparison of reaction rates with various substituents X (electron donors increased the rate).[1] Other mechanistic scenarios also seem consistent with the reported data, however. Two such possibilities are shown in Scheme 2: a stepwise mechanism with rate-determining aryl attack (mechanism B; donor substituents could accelerate this step by making the aryl group more nucleophilic) and a stepwise mechanism with rate-determining alkenyl shift (mechanism C; donor substituents could accelerate this step by through-space stabilization of the cationic substructure in the transition structure, a cation·π effect[3]).

SCHEME 1

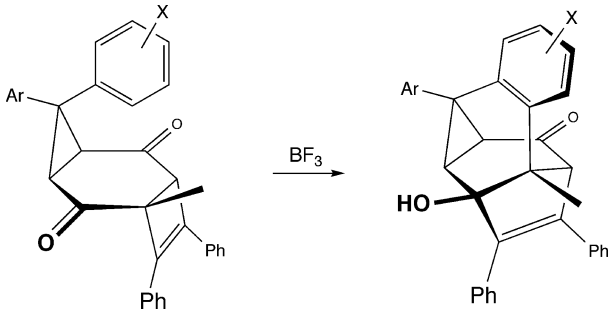

We have a general interest in unusual carbocation rearrangements,[4] as well as the ability of lone pairs and π-systems to stabilize delocalized cationic intermediates and transition structures via through-space interactions.[5] Consequently, we were intrigued by the unusual rearrangement in Scheme 1 and decided to explore its mechanism, using hybrid Hartree−Fock/density functional theory computations, with the goal of differentiating between possibilities A−C (Scheme 2).

(1) Koizumi, T.; Harada, K.; Mochizuki, E.; Kokubo, K.; Oshima, T. *Org. Lett.* **2004**, *6*, 4081−4084.

(2) (a) Koizumi, T.; Mochizuki, E.; Kokubo, K.; Oshima, T. *J. Org. Chem.* **2004**, *69*, 4577−4585. (b) Kokubo, K.; Koizumi, T.; Harada, K.; Mochizuki, E.; Oshima, T. *J. Org. Chem.* **2005**, *70*, 7776−7779. (c) Koizumi, T.; Harada, K.; Asahara, H.; Mochizuki, E.; Kokubo, K.; Oshima, T. *J. Org. Chem.* **2005**, *70*, 8364−8371.

(3) Reviews on cation·π interactions include: (a) Ma, J. C.; Dougherty, D. A. *Chem. Rev.* **1997**, *97*, 1303−1324. (b) Gokel, G. W. *Chem. Commun.* **2003**, 2847−2852.

(4) (a) Gutta, P.; Tantillo, D. J. *Angew. Chem., Int. Ed.* **2005**, *44*, 2719−2723. (b) Ho, G. A.; Nouri, D. H.; Tantillo, D. J. *J. Org. Chem.* **2005**, *70*, 5139−5143. (c) Wang, S. C.; Tantillo, D. J. *Eur. J. Org. Chem.* **2006**, 738−745. (d) Nouri, D. H.; Tantillo, D. J. *J. Org. Chem.* **2006**, *71*, 3686−3695. (e) Siebert, M. R.; Tantillo, D. J. *J. Org. Chem.* **2006**, *71*, 645−654. (f) Gutta, P.; Tantillo, D. J. *J. Am. Chem. Soc.* **2006**, *128*, 6172−6179. (g) Hong, Y. J.; Tantillo, D. J. *Org. Lett.* **2006**, *8*, 4601−4604. (h) Siebert, M. R.; Tantillo, D. J. *J. Phys. Org. Chem.* **2006**, *20*, 384−394. (i) Gutta, P.; Tantillo, D. J. *Org. Lett.* **2006**, *9*, 1069−1071.

10.1021/jo701550t CCC: $37.00
Published on Web 09/27/2007

SCHEME 2

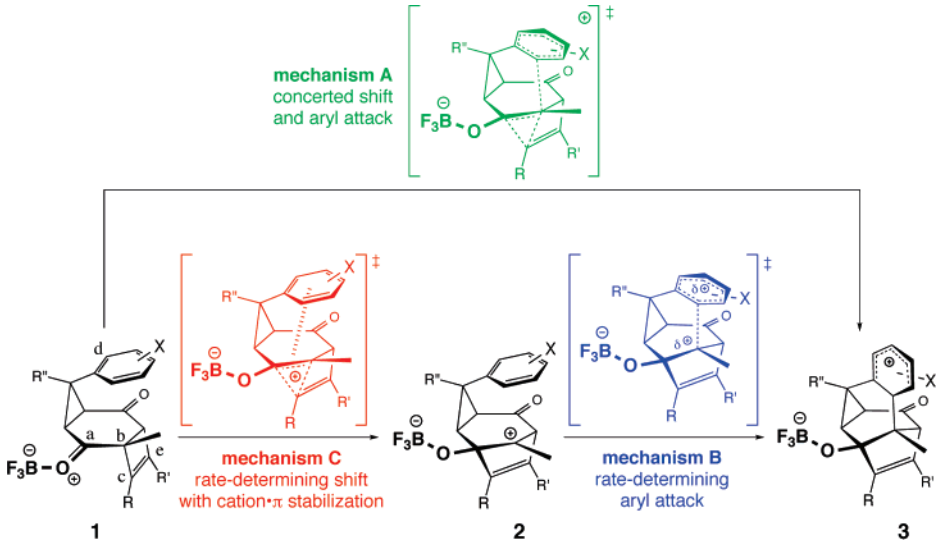

Methods

Gaussian03 was employed for all calculations.[6] Simplified model systems, in which three of the four aryl groups in the structures from Scheme 1 are replaced by hydrogens, were used for most calculations (Scheme 2, R = R′ = R″ = H, various X's = H, *m*-OMe, *m*-Me, *m*-Cl, *m*-CF_3, *m*-NH_2, *m*-NH_3^+, *m*-NO_2, *m*-CN, *p*-OMe, *p*-Me, *p*-Cl, *p*-CF_3, *p*-NH_2, *p*-NH_3^+, *p*-CN); exceptions are mentioned in the text.[7] All geometries were optimized using B3LYP/6-31G(d);[8] we and others have used B3LYP to describe carbocation rearrangements.[4] All stationary points were characterized as minima or transition structures by analyzing their vibrational frequencies (intrinsic reaction coordinate calculations[9a,b] were also carried out for the transition structures shown in Figure 1). All reported B3LYP/6-31G(d) energies include zero-point energy corrections from frequency calculations, scaled by 0.9806.[9c] In some cases, the effects of solvent were modeled using CPCM calculations (with UA0 radii),[10] a self-consistent reaction field (SCRF) method. Structural drawings were produced using *Ball & Stick*.[11]

Results and Discussion

Mechanism. Our studies began with the parent system, for which X = H, in the absence of solvent. If mechanism A (Scheme 2) is preferred for the reaction, we would expect to find a single transition structure connecting **1** and **3**. We could find no such transition structure, however, and instead found an intermediate, **2**, and two separate transition structures connecting it to **1** and **3** (Figure 1).[12,13] The same situation was observed for all substituents (X) that we explored (see Methods for list of substituents). Moreover, for all substituents examined, the aryl attack step is rate-determining, indicating that mechanism B predominates. Although mechanism A does not occur, we note that the difference in energy between the **1** → **2** transition structure and intermediate **2** is small.[14] Thus, there is only a subtle difference between this incarnation of mechanism B and a concerted but asynchronous version of mechanism A.

Oshima and co-workers described a correlation between reaction rates and Hammett σ constants for X = H, *m*-OMe, *m*-Me, *m*-Cl, *p*-OMe, *p*-Me, *p*-Cl, and *p*-CF_3.[1,7] We show in Figure 2 a plot of computed energy barriers (from **1** to the **2** → **3** transition structure) versus σ constants for various substituents.[15−17] In agreement with the experimental observations of Oshima and co-workers, the calculations predict that the **1** → **3** rearrangement should be faster with electron-donating

(5) (a) Bojin, M. D.; Tantillo, D. J. *J. Phys. Chem. A* **2006**, *110*, 4810−4816 and references therein. (b) Wang, S. C.; Tantillo, D. J. *J. Phys. Chem. A* **2007**, *111*, 7149−7153. (c) Hong, Y. J.; Tantillo, D. J. *J. Org. Chem.*, in press. (d) For leading references on intramolecular cation•π interactions implicated in controlling the stereochemistry of reactions of alkyl azides, see: Yao, L.; Aube, J. *J. Am. Chem. Soc.* **2007**, *129*, 2766−2767.

(6) Frisch, M. J.; Trucks, G. W.; Schlegel, H. B.; Scuseria, G. E.; Robb, M. A.; Cheeseman, J. R.; Montgomery, J. A., Jr.; Vreven, T.; Kudin, K. N.; Burant, J. C.; Millam, J. M.; Lyengar, S. S.; Tomasi, J.; Barone, V.; Mennucci, B.; Cossi, M.; Scalmani, G.; Rega, N.; Petresson, G. A.; Nakatsuji, H.; Hada, M.; Ehara, M.; Toyota, K.; Fukuda, R.; Hasegawa, J.; Ishida, M.; Nakajima, T.; Honda, Y.; Kitao, O.; Nakai, H.; Klene, M.; Li, X.; Knox, J. E.; Hratchian, H. P.; Cross, J. B.; Adamo, C.; Jaramillo, J.; Gomperts, R.; Stratmann, R. E.; Yazyev, O.; Austin, A. J.; Cammi, R.; Pomelli, C.; Ochterski, J. W.; Ayala, P. Y.; Morokuma, K.; Voth, G. A.; Salvador, P.; Dannenberg, J. J.; Zakrzewski, V. G.; Dapprich, S.; Daniels, A. D.; Strain, M. C.; Farkas, O.; Malick, D. K.; Rabuck, A. D.; Raghavachari, K.; Foresman, J. B.; Ortiz, J. V.; Cui, Q.; Baboul, A. G.; Clifford, S.; Cioslowski, J.; Stefanov, B. B.; Liu, G.; Liashenko, A.; Piskorz, P.; Komaromi, I.; Martin, R. L.; Fox, D. J.; Keith, T.; Al-Laham, M. A.; Peng, C. Y.; Nanayakkara, A.; Challacombe, M.; Gill, P. M. W.; Johnson, B.; Chen, W.; Wong, M. W.; Gonzalez, C.; Pople, J. A. *Gaussian03*, revision B.04; Gaussian, Inc.: Pittsburgh, PA, 2003.

(7) The meta/para nomenclature used herein describes the relative position of the substituents X and the final C−C bond that forms during the rearrangement, as shown for **3** below.

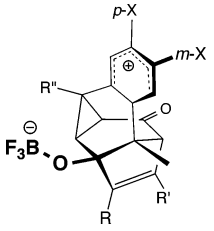

(8) (a) Becke, A. D. *J. Chem. Phys.* **1993**, *98*, 5648−5652. (b) Becke, A. D. *J. Chem. Phys.* **1993**, *98*, 1372−1377. (c) Lee, C.; Yang, W.; Parr, R. G. *Phys. Rev. B* **1988**, *37*, 785−789. (d) Stephens, P. J.; Devlin, F. J.; Chabalowski, C. F.; Frisch, M. J. *J. Phys. Chem.* **1994**, *98*, 11623−11627.

(9) (a) Gonzalez, C.; Schlegel, H. B. *J. Phys. Chem.* **1990**, *94*, 5523−5527. (b) Fukui, K. *Acc. Chem. Res.* **1981**, *14*, 363−368. (c) Scott, A. P.; Radom, L. *J. Phys. Chem.* **1996**, *100*, 16502−16513.

(10) (a) Barone, V.; Cossi, M. *J. Phys. Chem. A* **1998**, *102*, 1995−2001. (b) Barone, V.; Cossi, M.; Tomasi, J. *J. Comput. Chem.* **1998**, *19*, 404−417.

(11) Müller, N.; Falk, A. *Ball & Stick*, version 3.7.6, molecular graphics application for MacOS computers; Johannes Kepler University: Linz, Austria, 2000.

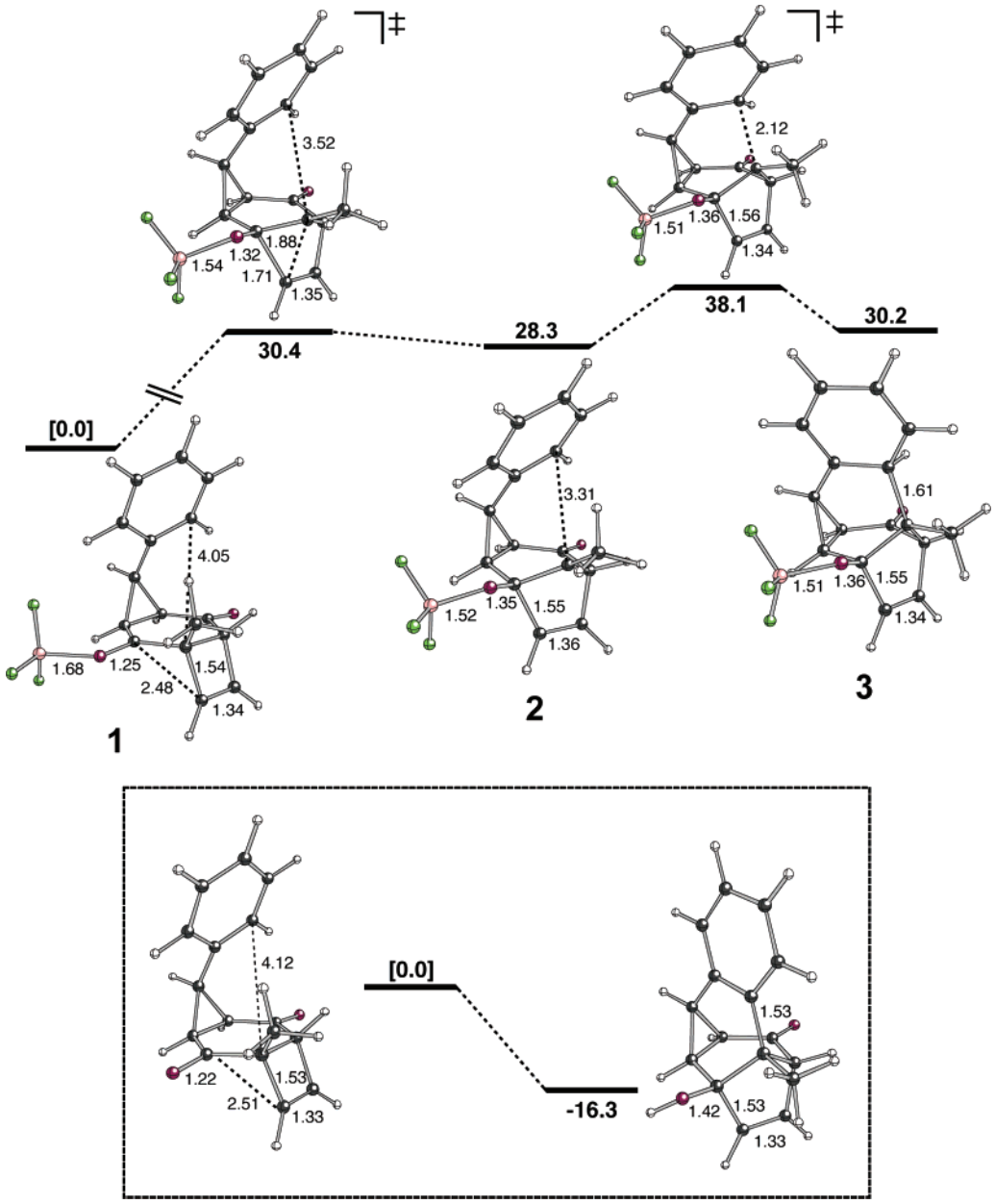

FIGURE 1. Top: geometries and relative energies (B3LYP/6-31G(d), distances in Å, energies in kcal/mol) for structures involved in the BF_3-catalyzed rearrangement.[14] Box at bottom: Energetics for the overall reaction (i.e., reactant and product without BF_3).

substituents. Consequently, a mechanism involving a concerted alkenyl shift and aryl attack (mechanism A) need not be invoked to explain the experimental data.

Solvent Effects. In their mechanistic study,[1] Oshima and coworkers examined several solvents. For comparison, we examined three of these: chloroform (which is also the solvent used in the original report for exploring substituent effects[1]), dichloromethane, and benzene. First, structures for the parent system (X = H) were reoptimized using chloroform as solvent (see Methods for details). The mechanism for the **1** → **3** rearrangement in chloroform does not differ significantly from that in the gas phase. The solvent does, however, interact more strongly with each successive stationary point along the reaction coordinate, leading to the following relative energies: **1**, [0.0] kcal/mol; **1** → **2** transition structure, 25.1 kcal/mol; **2**, 21.0 kcal/mol; **2** → **3** transition structure, 29.6 kcal/mol; **3**, 17.4 kcal/mol.[18] This is consistent with an increasing separation of charge as the reaction proceeds (i.e., the bulk of the positive charge moves further and further from the negatively charged OBF_3 group). The same system was also examined with dichloromethane and benzene. In dichloromethane, the following relative energies were obtained: **1**, [0.0] kcal/mol; **1** → **2** transition structure, 24.1 kcal/mol; **2**, 19.7 kcal/mol; **2** → **3** transition structure, 27.9 kcal/mol; and **3**, 15.1 kcal/mol. In benzene, the following energies were obtained: **1**, [0.0] kcal/mol; **1** → **2** transition structure, 27.3 kcal/mol; **2**, 23.7 kcal/mol; **2** → **3** transition structure, 32.6 kcal/mol; and **3**, 21.8 kcal/mol. These results suggest that, for the three solvents examined computationally, the reaction should be fastest in dichloromethane and slowest in benzene, which is in agreement with the relative rates reported by Oshima et al. (dichloromethane = 21, chloroform = 1.3, benzene = 1.0),[1] again indicating that

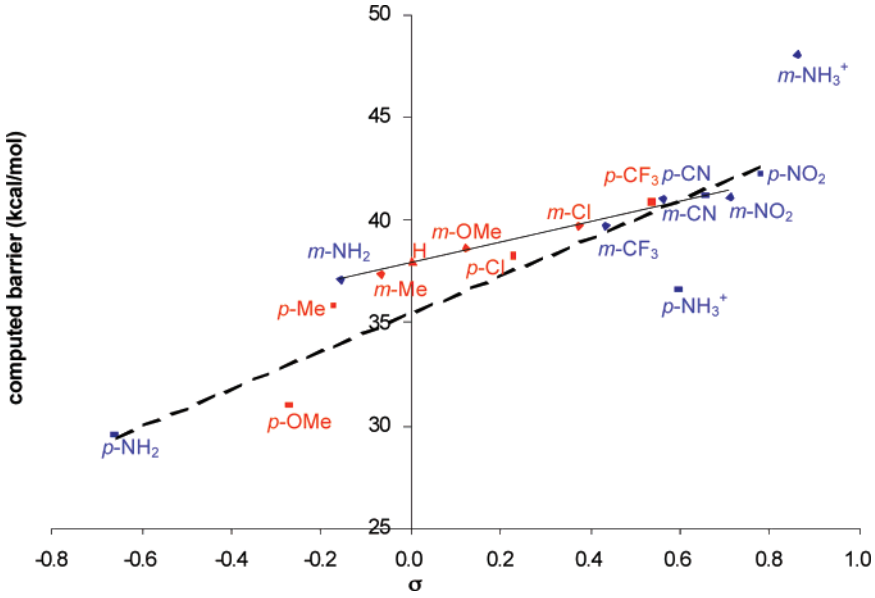

FIGURE 2. Plot of calculated barriers (from **1** to the **2** → **3** transition structure) for BF_3-catalyzed rearrangement versus Hammett constants (σ_m and σ_p).[16] The substituents shown in red are the ones used in the experiments of Oshima and co-workers,[1] and additional substituents that we examined are shown in blue. Substituents at the meta position are indicated by diamonds, whereas those at the para position are indicated by squares.[7] The straight full line corresponds to the meta substituents, excluding *m*-NH_3^+, whereas the dashed line corresponds to the para substituents, excluding *p*-NH_3^+.[17]

a concerted mechanism need not be invoked to explain the experimental data.

Substituent Effects on BF_3 Complexation. We were curious as to whether the electron-donating and -withdrawing properties of the relatively remote substituents X had any significant effect on the complexation of the reactant by BF_3 (to produce **1**) and therefore possibly on the barriers for rearrangement if separate BF_3 and ketone reactants were used as a starting point. The computed complexation energies (**1** vs separate BF_3 and ketone reactant) generally vary from 10 to 15 kcal/mol (in the gas phase, where any effects are likely to be largest). From Figure 3, one can see that the magnitude of the complexation energy is slightly larger with electron-donating substituents. This small difference may arise from a direct through-space interaction between the aromatic ring and the carbonyl (which could involve the aromatic π and carbonyl π^* orbitals and/or simple electrostatic

(12) A conformer of **1** (shown below) where the BF_3 group points towards the cyclobutene group was also located. This structure is ~4 kcal/mol higher in energy than structure **1** (Figure 1), and consequently we focus our discussion throughout the text on conformers that have their BF_3 group oriented as shown in Figure 1 rather than as in the structure below. See Supporting Information for additional details.

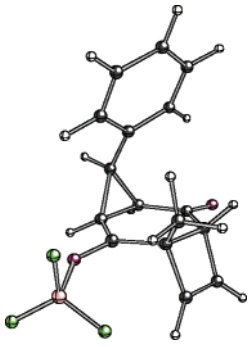

(13) Although the overall barrier for the **1** to **3** reaction appears to be too high to be consistent with the reaction conditions described in ref 1, it does not include the effects of reactant complexation by BF_3 (vide infra).

(14) Since the energy difference between the first transition structure (**1** → **2**) and intermediate **2** is rather small, structures **1** and **2** and the transition structure connecting them were also optimized with B3LYP/6-311+G(d,p); extremely similar results were obtained at this level of theory: **2** is 26.4 kcal/mol less stable than **1**, and the transition state connecting **1** and **2** is 28.9 kcal/mol higher in energy than **1**. Full optimizations at the MP2/6-31G(d) level gave qualitatively similar results: 0.0 kcal/mol (**1**), 26.2 (**1** → **2**), 23.6 (**2**), 30.0 (**2** → **3**), 24.7 (**3**). See Supporting Information for additional details.

(15) For each substituent, we were able to locate two transition-state structures for the **2** → **3** step, differing in the orientation of the aromatic ring and which of its carbons is attacked (see below). Transition structures with H2 "in front" (below, right) are generally 1−5 kcal/mol higher in energy than those with H1 "behind" (below, left; Scheme 2; Figure 1). In addition, the transition structures with H2 "in front" do not seem to lead to minima analogous to **3**. Instead, rearomatization appears to occur directly from deprotonation via one of the fluorines on the nearby BF_3 group. It is unlikely that this would occur in solution, however. For these reasons, H2 "in front" structures are not discussed further. See Supporting Information for additional details.

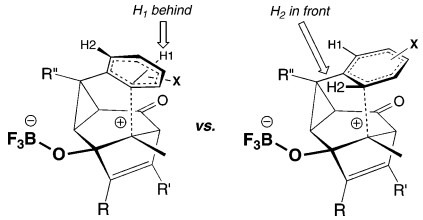

(16) Hansch, C.; Leo, A.; Taft, R. W. *Chem. Rev.* **1991**, *91*, 165−195.

(17) Ammonium substituents were excluded from the best-fit lines since these are the only substituents examined that bear a full charge, and intramolecular interactions between the NH_3^+ and BF_3 groups were observed in some structures, leading to geometries that are unlikely in solution (see Supporting information for details).

(18) While the minima and transition structures were fully optimized in our solvent calculations, troubles were encountered in achieving convergence for some accompanying frequency calculations. Therefore, zero-point corrections were not included for the numbers presented here. Test calculations with $CHCl_3$ were performed, and these verified that zero-point corrections do not affect the results significantly.

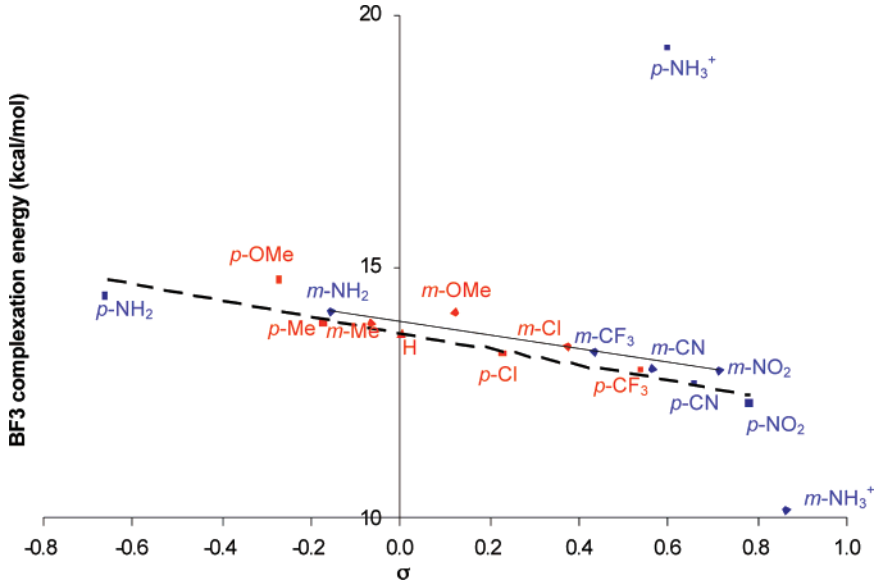

FIGURE 3. Plot of absolute magnitude of the calculated BF_3 complexation energy for the reactant ketone versus Hammett constants (σ_m and σ_p).[16] The substituents shown in red are the ones used in the experiments of Oshima and co-workers,[1] and additional substituents that we examined are shown in blue. Substituents at the meta position are indicated by diamonds, whereas those at the para position are indicated by squares.[7] The straight full line corresponds to the meta substituents, excluding *m*-NH_3^+, whereas the dashed line corresponds to the para substituents, excluding *p*-NH_3^+.[17]

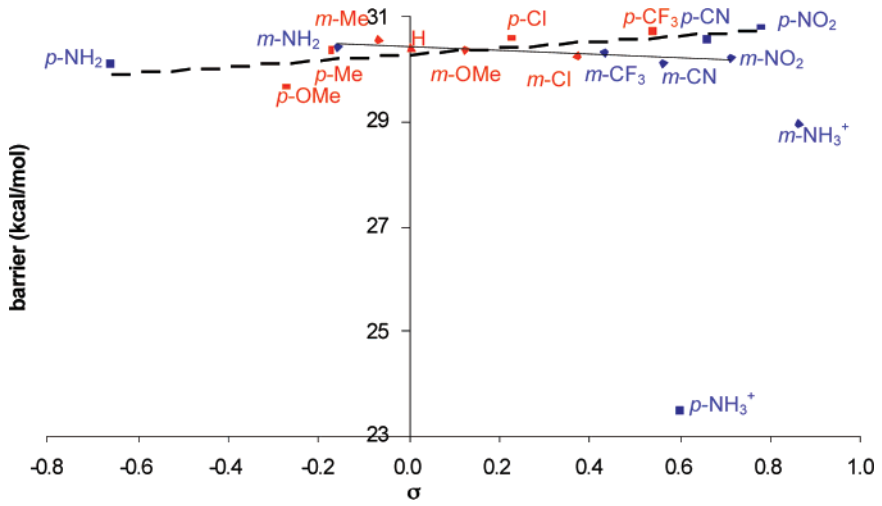

FIGURE 4. Plot of calculated barriers from **1** to the **1** → **2** transition structure versus Hammett constants (σ_m and σ_p).[16] The substituents shown in red are the ones used in the experiments of Oshima and co-workers,[1] and additional substituents that we examined are shown in blue. Substituents at the meta position are indicated by diamonds, whereas those at the para position are indicated by squares.[7] The straight full line corresponds to the meta substituents, excluding *m*-NH_3^+, whereas the dashed line corresponds to the para substituents, excluding *p*-NH_3^+.[17]

attraction), which should be stronger when the carbonyl is complexed to the Lewis acidic BF_3.

Cation·π Effects on the [1,2] Alkenyl Shift. Although our calculations indicate that the alkenyl shift is not the rate-determining step of the reaction, we were still curious as to whether there might be some sort of intramolecular cation·π interaction that affects the barrier for this step.[3] We were particularly interested in such issues since many carbocation rearrangements occurring in nature could possibly involve cation·π interactions between bridged carbocation intermediates or transition structures and aromatic residues in enzyme active sites.[4,5a] If cation·π interactions between the aromatic ring and the positive charge spread over the migrating alkenyl group, C_a and C_b (Scheme 2, structure **1** for labels) are stronger than the aromatic ring → carbonyl interactions for **1** described earlier (which can also be described as a sort of cation·π interaction), the barrier for the **1** → **2** step should be lower for donor substituents than it is for acceptor substituents. In addition, such interactions should also lead to shorter distances between the aromatic ring and the carbons involved in the [1,2] shift for donor substituents than for acceptor substituents. Computed barriers for the **1** → **2** step are plotted versus σ constants in Figure 4. There appears to be only a very slight dependence of the barrier height on the electron-donating or -withdrawing ability of the substituent. For the para substituents, the barriers are very slightly lower with donor substituents than with accepting groups. For the meta substituents, this dependence is essentially nonexistent. This suggests that any through-space interactions between the aromatic ring and C_a or C_b are, at most, only very slightly stronger in the **1** → **2** transition structure than

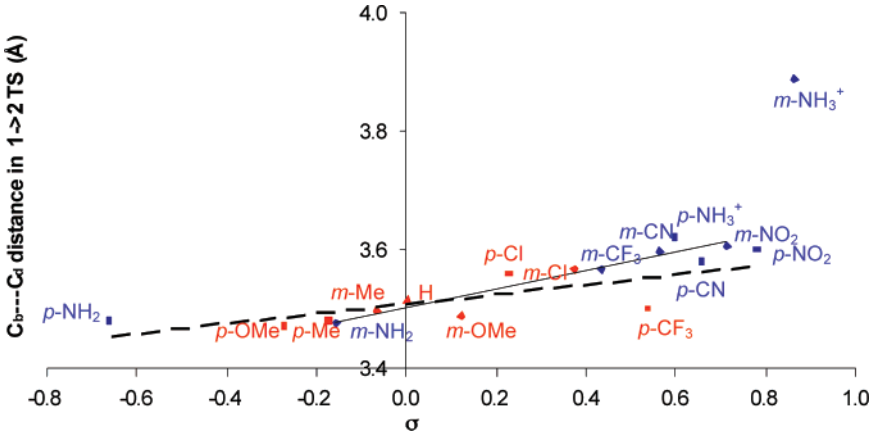

FIGURE 5. Plots of aryl---cation (C_b---C_d in Scheme 2) distance (Å) in transition structures for the **1** → **2** step versus Hammett constants (σ_m and σ_p).[16] The substituents shown in red are the ones used in the experiments of Oshima and co-workers,[1] and additional substituents that we examined are shown in blue. Substituents at the meta position are indicated by diamonds, whereas those at the para position are indicated by squares.[7] The straight full line corresponds to the meta substituents, excluding *m*-NH_3^+, whereas the dashed line corresponds to the para substituents, excluding *p*-NH_3^+.[17]

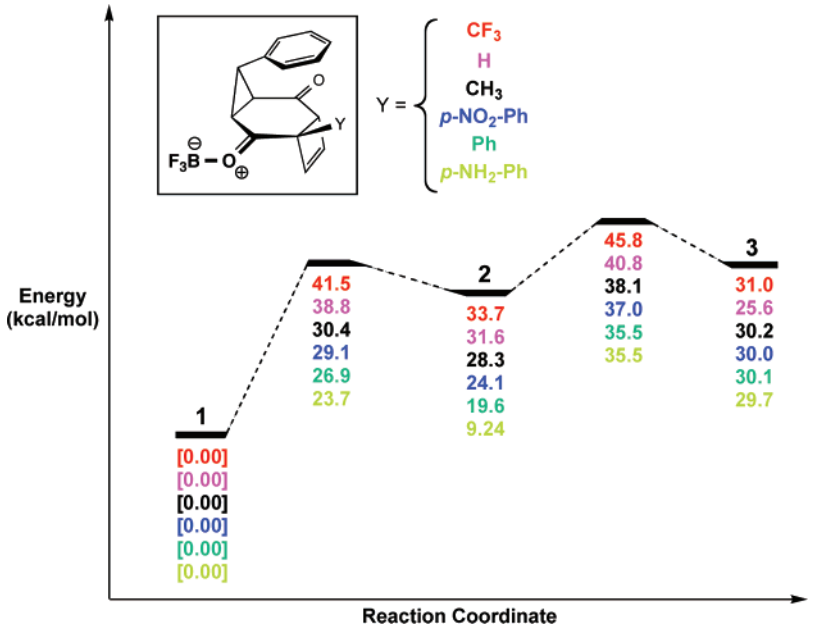

FIGURE 6. Computed relative energies (kcal/mol) of stationary points for systems with various substituents Y.

in **1**. Figure 5 shows that there is also only a small dependence of the C_b-C_d distance on σ.

Role of the Methyl Group. The role of the methyl group attached to C_b was probed by replacing the methyl with various groups having different electronic properties. The energies of the stationary points for the **1** → **3** reaction with a variety of attached groups (Y) are shown in Figure 6. As expected, species with significant positive charge at C_b are selectively stabilized by both the methyl and aryl groups compared to Y = H. The electron-withdrawing CF_3 group has the opposite effect. Not surprisingly, intermediate **2** is most sensitive to the electron-donating or -withdrawing ability of the attached group. This sensitivity to substituents provides an additional avenue for increasing the facility of the rearrangement and could be probed through future experiments.

Roles of the Phenyl Groups. We were also curious about the effects of phenyl groups attached directly to the migrating alkenyl group in the **1** → **2** step since the systems explored by Oshima and co-workers had phenyl groups at both C_c or C_e (Scheme 1). The results of our calculations with and without phenyl groups at C_c and/or C_e are summarized in Figures 7 and 8.

The presence of phenyl groups at C_c or C_e affects the barriers for the [1,2] alkenyl shift: having a phenyl group at C_c increases the barrier by ~2−6 kcal/mol, and having a phenyl group at C_e decreases the barrier for the [1,2] shift by ~2 kcal/mol. Although the origins of these counterbalancing effects are not entirely clear and likely result from the combination of several small effects, some interesting geometric changes occur during the rearrangement. For example, in cases where there is a phenyl group at C_c, this group is more nearly coplanar with the C_c═C_e double bond in **1** and **2** ($C_e-C_c-C_{Ph,ipso}-C_{Ph,ortho} \leq 22°$) than in the **1** → **2** transition structure ($C_e-C_c-C_{Ph,ipso}-C_{Ph,ortho}$ increases by 30−40°). This perhaps indicates an effort on the

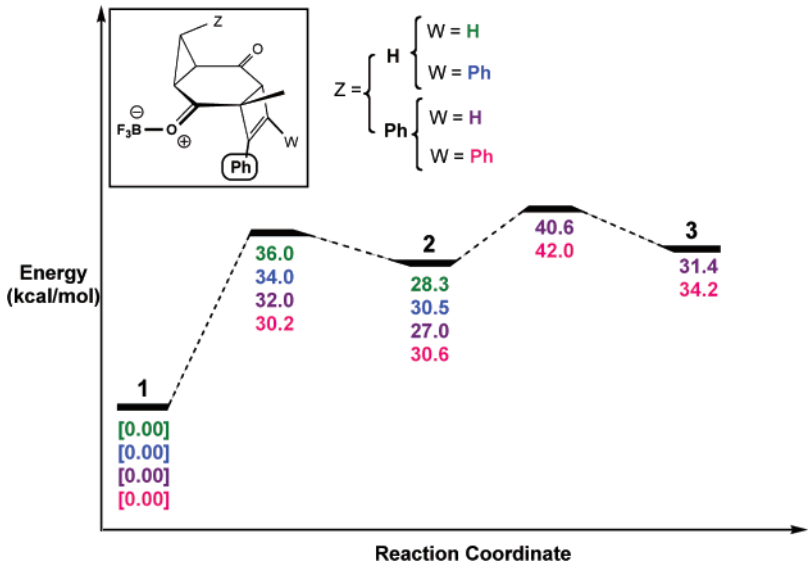

FIGURE 7. Computed relative energies (kcal/mol) of stationary points for systems with and without Z and W = Ph and a phenyl group at C_c. Note that, for Z = Ph, W = Ph, **2** is actually very slightly higher in energy than the **1** → **2** transition structure when zero-point energy corrections are included.

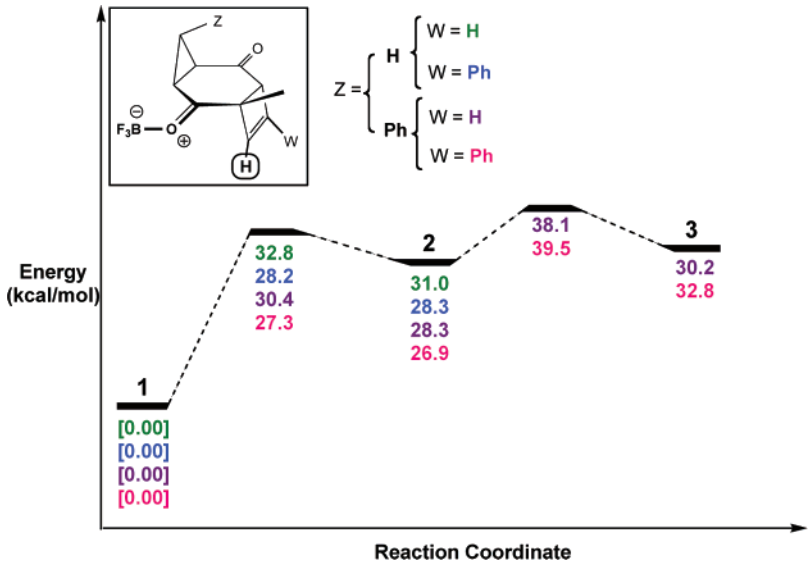

FIGURE 8. Computed relative energies (kcal/mol) of stationary points for systems with and without Z and W = Ph and a hydrogen at C_c.

part of the phenyl group to delocalize the positive charge that is building up at C_c as it migrates, but given that the presence of the phenyl group increases the barrier, this effect must be smaller than favorable interactions involving the phenyl group in **1**.

Note also that, for the largest system we explored (that with three phenyl groups (Figure 7, W = Z = Ph) and the one closest to the experimental system explored by Oshima and co-workers), the energy of **2** is very slightly higher than that of the transition structure for its formation when zero-point energy corrections are included, implying that this reaction is effectively concerted (at least in the absence of solvent), but that the [1,2] shift and attack of the aromatic ring occur extremely asynchronously (a similar situation is observed for the system with only one phenyl group, that at C_e).

Are the Intermediates Nonclassical Cations? Given the proximity of the carbocationic centers (C_b) and the C_c═C_e double bonds in intermediates **2**, we wondered whether there might be a three-center two-electron interaction between these groups (Chart 1) of the sort found in corner-protonated cyclopropanes, the prototypical class of nonclassical cations.[19] Let us consider several geometric parameters relevant to this issue. For the intermediates **2** examined herein, C_b−C_c and C_b−C_e distances ranged from 1.76 to 2.41 Å, C_c═C_e distances ranged from 1.33 to 1.41 Å, and C_b−C_a−C_c angles ranged from 76 to

CHART 1

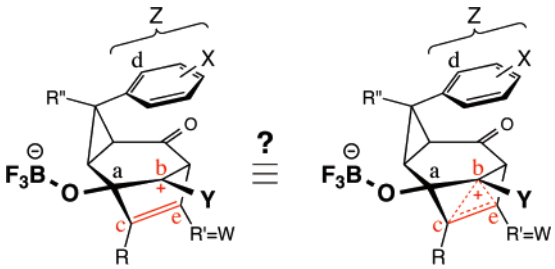

101° (see Table S1 in the Supporting Information for details). Clearly, some of these structures have considerable three-center interactions; in fact, many have $C_b-C_{c/e}$ distances ≤ 2 Å, $C_c=C_e$ distances ≥ 1.35 Å, and $C_b-C_a-C_c$ angles ≤ 85°, geometric parameters that are typical of nonclassical carbocations of the corner-protonated cyclopropane type,[4b,19] and, not surprisingly, the strength (judged on the basis of these geometric criteria) and symmetry of the $C_c-C_b-C_e$ interactions are modulated by groups directly attached to C_b, C_c, C_e.

Moreover, the geometry of the $C_c-C_b-C_e$ array is also very sensitive to the identity of the aromatic group Z, with stronger three-center interactions being observed for systems with electron-withdrawing X groups. For example, for X = *m*-NH_3^+, a strong electron-withdrawing group, the distance between C_b and the aromatic ring is long (C_b-C_d = 3.88 Å) and C_b and the $C_c=C_e$ group appear to interact strongly (C_b-C_c = 1.90 Å, C_b-C_e = 1.85 Å, $C_c=C_e$ = 1.38 Å, and $\angle C_b-C_a-C_c$ = 77°). In contrast, for X = *m*-NH_2, a strong electron-donating group, the distance between C_b and the aromatic ring is short (C_b-C_d = 2.54 Å) and C_b and the $C_c=C_e$ group are relatively far apart (C_b-C_c = 2.40 Å, C_b-C_e = 2.38 Å, $C_c=C_e$ = 1.33 Å, and $\angle C_b-C_a-C_c$ = 101°). Thus, our calculations strongly suggest that through-space cation·π interactions[3] between the aromatic ring and C_b can modulate the nonclassical character of corner-protonated cyclopropanes, a phenomenon that would be worth exploring through additional structural studies.

These systems are quite complex, however, and a competition actually exists between the aromatic ring Z, the $C_c=C_e$ π-bond, and the Y group for delocalization of the positive charge at C_b, a competition whose outcome is influenced by both the electron-donating ability of each group and its ability to interact strongly with C_b without inducing severe geometric strain. Consider, for example, the Y = CH_3 and Y = Ph cases (both with Z = Ph, R = R′ = R″ = H as shown in Figure 6). With Y = CH_3, C_b and the $C_c=C_e$ group interact fairly strongly (C_b-C_c = 2.04 Å, C_b-C_e = 2.03 Å, $C_c=C_e$ = 1.36 Å, $\angle C_b-C_a-C_c$ = 84°, and C_b-C_d = 3.30 Å), whereas with Y = Ph, a group that is much better at delocalizing a positive charge through direct π-donation, C_b interacts less strongly with both the $C_c=C_e$ group and the aromatic ring Z (C_b-C_c = 2.23 Å, C_b-C_e = 2.24 Å, $C_c=C_e$ = 1.34 Å, $\angle C_b-C_a-C_c$ = 93°, and C_b-C_d = 3.38 Å), consistent with there being a smaller "electron demand"[20] at C_b when the phenyl group replaces the methyl group. Now consider the corresponding Y = CF_3 case: here the strongly electron-withdrawing CF_3 group increases the electron demand at C_b, but this leads to a stronger cation·π interaction at the expense of the three-center (nonclassical) interaction (C_b-C_c = 2.41 Å, C_b-C_e = 2.40 Å, $C_c=C_e$ = 1.33 Å, $\angle C_b-C_a-C_c$ = 101°, and C_b-C_d = 2.57 Å). There is indeed a complex interplay between direct (hyper)conjugation (with Y), intramolecular cation·π interactions (through-space with the aromatic ring Z), and three-center "nonclassical" stabilization (through-space with the $C_c=C_e$ π-bond) for these structures as they strive to slake C_b's thirst for electron density.

Conclusions

Quantum mechanical calculations were used to study the concertedness of and substituent effects on the alkenyl migration/electrophilic aromatic substitution reaction developed by the Oshima group. For all substituents examined, our calculations suggest that a stepwise mechanism with a rate-determining aryl attack step (mechanism B in Scheme 2) prevails, although the intermediate involved, which often sports considerable "nonclassical ion character", generally does not reside in a very deep minimum, making the reaction effectively concerted for some cases.

Acknowledgment. We gratefully acknowledge the University of California, Davis, the donors of the American Chemical Society's Petroleum Research Fund, and the National Science Foundation (CAREER program and computer time from the Pittsburgh Supercomputer Center) for support.

Supporting Information Available: Coordinates and energies for all structures and additional details on calculations. This material is available free of charge via the Internet at http://pubs.acs.org.

JO701550T

(19) For leading references on nonclassical ions, see: (a) Grob, C. A. *Acc. Chem. Res.* **1983**, *16*, 426−431. (b) Brown, H. C. *Acc. Chem. Res.* **1983**, *16*, 432−440. (c) Olah, G. A.; Prakash, G. K. S.; Saunders, M. *Acc. Chem. Res.* **1983**, *16*, 440−448. (d) Walling, C. *Acc. Chem. Res.* **1983**, *16*, 448−454. (e) Brown, H. C. *The Nonclassical Ion Problem;* Plenum: New York, 1977. For X-ray crystal structures, see: (f) Laube, T. *Acc. Chem. Res.* **1995**, *28*, 399−405.

(20) For leading references on the "tool of increasing electron demand", see: Olah, G. A.; Berrier, A. L.; Prakash, G. K. S. *Proc. Natl. Acad. Sci. U.S.A.* **1981**, *78*, 1998−2002.